

REPRODUCTION  
COPY

# LOS ALAMOS SCIENTIFIC LABORATORY

OF THE UNIVERSITY OF CALIFORNIA  
LOS ALAMOS, NEW MEXICO

CONTRACT W-7405-ENG.36 WITH THE  
U.S. ATOMIC ENERGY COMMISSION

LOS ALAMOS NATIONAL LABORATORY  
  
3 9338 00407 4075

DATA

THE ATOMIC ENERGY ACT OF 1946. ITS TRANSMITTAL  
BY AN UNAUTHORIZED PERSON IS PROHIBITED.

UNCLASSIFIED

LOS ALAMOS SCIENTIFIC LABORATORY  
of the  
UNIVERSITY OF CALIFORNIA

Report written:  
January 20, 1955

LAMS-1902 This document consists of 36 pages

0.3

PHOTOGRAMMETRIC PROBLEMS ASSOCIATED  
WITH  
NUCLEAR DETONATION TEST EXPERIMENTS

by

D. F. Seacord, Jr.

SPECIAL REREVIEW	Reviewers	Class.	Date
FINAL	NPR	U	6/20/79
DETERMINATION	SHU	U	4/7/82
Class: <u>U</u>			

LOS ALAMOS NATL. LAB. LIBS.  
3 9338 00407 4075

All Los Alamos reports present the opinions of the author or authors and do not necessarily reflect the views of the Los Alamos Scientific Laboratory. Furthermore, this LAMS report has not been prepared for general distribution. It is accordingly requested that no distribution be made without the permission of the Director's Office of the Laboratory.

UNCLASSIFIED

UNCLASSIFIED



UNCLASSIFIED



Report distributed: JUN 8 1955

LAMS-1902

AEC Classified Technical Library  
University of California Radiation Laboratory, Livermore  
Edgerton, Germeshausen & Grier, Inc., Boston  
Los Alamos Report Library

1-7  
8  
9  
10-40

**PUBLICLY RELEASABLE**

Per Mark M. Jones ESS-16 Date: 10-27-95  
By Marcia Ballejo CIC-14 Date: 11-8-95

**VERIFIED UNCLASSIFIED**

Per NPA 6-20-79  
By Marcia Ballejo 11-8-95

Classification changed to UNCLASSIFIED  
by authority of the U. S. Atomic Energy Commission.  
For ADR(TID-1400-S2) Sept-Oct 1974  
By REPORT LIBRARY Judy Garcia 7-25-75

UNCLASSIFIED



UNCLASSIFIED

  
UNCLASSIFIEDABSTRACT

Photogrammetric analysis of object position and displacement in two and three dimensions is outlined. Extension to problems arising in the photographic documentation of the rate of growth of an explosion fireball are indicated.

UNCLASSIFIED

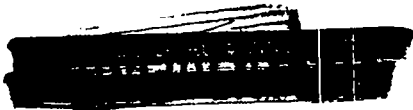


UNCLASSIFIED

CONTENTS

	<u>Page</u>
SECTION I INTRODUCTION. . . . .	6
SECTION II TWO-DIMENSIONAL DISPLACEMENT OF A POINT .	7
SECTION III THREE-DIMENSIONAL DISPLACEMENT OF A POINT. . . . .	13
SECTION IV FIREBALL PHOTOGRAMMETRY . . . . .	17
A. Surface Burst	
B. Air Burst	
a) Triangulation	
b) Magnification Factor	
c) Apparent Radius vs. True Radius	
d) Distortion of Image Due to Geometry	

UNCLASSIFIED



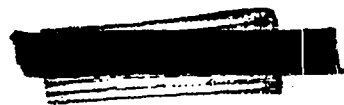


SECRET

ILLUSTRATIONS

		<u>Page</u>
FIGURE 1	OBJECT DISPLACEMENT NOT CROSSING OPTIC AXIS. . . . .	26
FIGURE 2	OBJECT DISPLACEMENT ACROSS OPTIC AXIS . . .	27
FIGURE 3	MEASURED FILM HEIGHT vs. OBJECT HEIGHT. . .	28
FIGURE 4	THREE-DIMENSIONAL DISPLACEMENT, ELEVATION .	29
FIGURE 5	THREE-DIMENSIONAL DISPLACEMENT, PLAN. . . .	30
FIGURE 6	TRUE vs. APPARENT FIREBALL RADIUS, SURFACE BURST . . . . .	31
FIGURE 7	TRIANGULATION FOR BURST POINT . . . . .	32
FIGURE 8	TRUE HEIGHT OF BURST. . . . .	33
FIGURE 9	MAGNIFICATION FACTOR. . . . .	34
FIGURE 10	APPARENT vs. TRUE RADIUS, AIR BURST, VERTICAL PROJECTION . . . . .	35
FIGURE 11	APPARENT vs. TRUE RADIUS, AIR BURST, HORIZONTAL PROJECTION . . . . .	36

UNCLASSIFIED



~~CONFIDENTIAL~~

UNCLASSIFIED

PHOTOGRAMMETRIC PROBLEMS ASSOCIATED  
WITH NUCLEAR DETONATION TEST EXPERIMENTS

I. INTRODUCTION

With the advent of the IASL mass-motion experiments on Operation Buster/Jangle the problem of photogrammetric analysis became of direct importance to Group J-10 in the reduction of photographic data.

The conversion of position and displacement, as measured on the photographic record, to the true spatial position and displacement, involved the photogrammetric technique in two dimensions (since the measured objects were approximately in the same horizontal plane as the nuclear detonation and the camera). Since the object displacements were small in comparison to the camera field of view, a simple cosine correction sufficed for translating film measurements to true displacement. This method was successfully applied to the results of both Operation Buster/Jangle and Operation Tumbler/Snapper.

However, large-scale detonations such as those in Operation Ivy, wherein displacements were comparable to the field of view, required a more refined correction factor. Furthermore, with the extension of the mass-motion experiment to high altitudes, the problem came to include three-dimensional photogrammetry.

The extension of this type of analysis to photographic data in fields other than mass motion became apparent with the application of the analytic solution to fireball data in the determination of the total hydrodynamic yield. Since the above method is theoretically capable of an accuracy of better than  $\pm 1\%$  in yield, the error in measured fireball

UNCLASSIFIED

~~CONFIDENTIAL~~

UNCLASSIFIED

UNCLASSIFIED



diameter must be reduced to the order of  $\pm 0.2\%$ . As groundwork for the future improvement in basic fireball data for the analytic solution, it was felt necessary to derive the photogrammetric equations for correcting the observed fireball diameter to its true diameter.

The derivations which follow are based on several simplifying assumptions: (1) lens distortion is negligible, (2) the object range is such that atmospheric refraction effects may be neglected, and (3) curvature of the earth is not taken into account (except where specifically noted).

## II. TWO-DIMENSIONAL DISPLACEMENT OF A POINT

The photogrammetric analysis for four cases involving the displacement of a point in two dimensions (i.e., optic axis horizontal and displacement in the horizontal plane) were involved in the data analysis from Operation Ivy, and are presented in the following sections. In general, the optic axis is not perpendicular to the line of object displacement in the region where the displacement occurs; this is usually dictated by the restrictions imposed on the location of object and camera.

Figure 1 is applicable to Cases A and B. The nuclear detonation point is designated Z, the camera, C, and the initial position of the object, O. (The experimental description may be stated briefly: the shock wave, expanding from Z, causes O to be displaced along line D.L.; the recorded film displacement  $x_1$  is to be related to the true spatial displacement  $y_1$ ). The problem is, of course, symmetrical about the optic axis but "left" and "right" will be used in a sense compatible with the figure.

Case A: The object is displaced from its initial position towards the optic axis but does not reach the optic axis. Referring to Figure 1, the following parameters are known:

UNCLASSIFIED

UNCLASSIFIED

$f$  = camera lens focal length

$R_z$  = range from camera to detonation point

$x_1$  = displacement as measured on film

$\phi$  = angle between displacement line and line connecting detonation point and camera

$(\beta + \gamma)$  = angle between optic axis and line from camera to initial position of object

$\alpha$  = angle between line from camera to initial position of object and line from camera to detonation point

$\theta$  = angle between displacement line and line from initial position of object to camera

It is desired to find  $y_1$ , the true spatial displacement, in terms of the above parameters.

$$\frac{y_1}{\sin \beta} = \frac{R_{p2}}{\sin \theta}, \quad \frac{x_1}{\sin \beta} = \frac{v_2}{\sin [90 - (\beta + \gamma)]}$$

or:

$$y_1/x_1 = \frac{R_{p2} \cos (\beta + \gamma)}{v_2 \sin \theta} \quad (A-1)$$

$R_{p2}$  and  $v_2$  are variables and may be replaced by equations relating them to known parameters.

$$\frac{R_{p2}}{v_2} = \frac{R_c + z_2}{f} = \frac{R_c + (y - y_1) \sin \psi}{f} \quad (A-2)$$

since  $z_2 = y_2 \sin \psi = (y - y_1) \sin \psi$ , where  $y = y_1 + y_2$

But:

$$\psi = 90 - (\beta + \gamma + \theta) \quad (A-3)$$

$$y = \frac{R_c \sin (\beta + \gamma)}{\sin \theta} \quad (A-4)$$

Substituting A-3 and A-4 in A-2:

$$\frac{R_{p2}}{v_2} = \frac{R_c + \left[ \frac{R_c \sin (\beta + \gamma)}{\sin \theta} - y_1 \right] \cos (\beta + \gamma + \theta)}{f} \quad (A-5)$$

UNCLASSIFIED

and substituting A-5 in A-1:

$$\frac{y_1}{x_1} = \frac{\left\{ R_c + \left[ \frac{R_c \sin(\beta+\gamma)}{\sin \theta} - y_1 \right] \cos(\beta+\gamma+\theta) \right\} \cos(\beta+\gamma)}{f \sin \theta} \quad (\text{A-6})$$

$R_c$  is related to  $R_z$  by:

$$R_c = \frac{R_z \sin \phi}{\sin(\alpha+\beta+\gamma+\phi)} \quad (\text{A-7})$$

Simplifying (A-6) and replacing  $R_c$  by (A-7):

$$y_1 = \frac{x_1 R_z \sin \phi \cos(\beta+\gamma) [1 + \sin(\beta+\gamma) \cos(\beta+\gamma+\theta) \csc \theta]}{\sin \theta \sin(\alpha+\beta+\gamma+\phi) [f + x_1 \cos(\beta+\gamma) \cos(\beta+\gamma+\theta) \csc \theta]} \quad (\text{A-8})$$

It may be seen that, if the optic axis is perpendicular to the line of displacement,  $\cos(\beta+\gamma+\theta) = 0$  and A-8 reduces to:

$$y_1 = \frac{x_1 R_z \sin \phi \cos(\beta+\gamma)}{f \sin \theta \sin(\alpha+\beta+\gamma+\phi)} \quad (\text{A-8a})$$

**CASE B:** The object is displaced from its initial position up to the optic axis. Figure 1 applies to Case B with:

$$y = y_1 + y_2$$

$$x = x_1 + x_2$$

$$\frac{y}{\sin(\beta+\gamma)} = \frac{R_c}{\sin \theta} \quad (\text{B-1})$$

$$\frac{x}{\sin(\beta+\gamma)} = \frac{f}{\cos(\beta+\gamma)} \quad (\text{B-2})$$

and

$$\frac{R_c}{\sin \phi} = \frac{R_z}{\sin(\alpha+\beta+\gamma+\phi)} \quad (\text{B-3})$$

Dividing B-1 by B-2 and substituting  $R_c$  of B-3:

$$y = \frac{x R_z \sin \phi \cos (\beta + \gamma)}{f \sin \theta \sin (\alpha + \beta + \gamma + \phi)} \quad (B-4)$$

In contrast to A-8a, the above equation is valid whether or not the optic axis is perpendicular to the line of displacement.

CASE C: The object is displaced from its initial position up to and across the optic axis but not to the perpendicular line of sight.

Figure 2 illustrates this case with the displacement to the right of the optic axis designated by "V". From the figure:

$$\frac{V}{\sin \eta} = \frac{R_{p2}}{\sin (\alpha + \beta + \gamma + \phi)} \quad (C-1a)$$

$$\sin \eta = x' / w_2 \quad (C-1b)$$

$$\frac{R_{p2}}{w_2} = \frac{R_c - z_1}{f} \quad (C-1c)$$

$$R_c = \frac{R_z \sin \phi}{\sin (\alpha + \beta + \gamma + \phi)} \quad (C-1d)$$

$$z_1 = V \cos (\alpha + \beta + \gamma + \phi) \quad (C-1e)$$

Substituting C-1b through C-1e in C-1a and solving for V:

$$V = \frac{x' R_z \sin \phi}{\sin (\alpha + \beta + \gamma + \phi) [f \sin (\alpha + \beta + \gamma + \phi) + x' \cos (\alpha + \beta + \gamma + \phi)]} \quad (C-2)$$

From Case B:

$$y = \frac{x R_z \sin \phi \cos (\beta + \gamma)}{f \sin \theta \sin (\alpha + \beta + \gamma + \phi)} \quad (C-3)$$

Adding C-2 and C-3:

$$y + V = \frac{R_z \sin \phi}{\sin (\alpha + \beta + \gamma + \phi)} \left[ \frac{x \cos (\beta + \gamma)}{f \sin \theta} + \frac{x'}{f \sin (\alpha + \beta + \gamma + \phi) + x' \cos (\alpha + \beta + \gamma + \phi)} \right] \quad (C-4)$$

CASE D: The object is displaced from its initial position, across the optic axis, and up to the perpendicular line of sight. Consider  $V'$  and  $x''$  of Figure 2:

$$\frac{V'}{R_{p2}} = \tan \eta = x''/f \quad (D-1)$$

$$R_{p2} = R_z \sin \phi \quad (D-2)$$

Combining D-1 and D-2:

$$V' = \frac{x'' R_z \sin \phi}{f} \quad (D-3)$$

Again, from Case B:

$$y = \frac{x R_z \sin \phi \cos (\beta + \gamma)}{f \sin \theta \sin (\alpha + \beta + \gamma + \phi)} \quad (D-4)$$

Adding:

$$y + V' = \frac{R_z \sin \phi}{f} \left[ \frac{x \cos (\beta + \gamma)}{\sin \theta \sin (\alpha + \beta + \gamma + \phi)} + x'' \right] \quad (D-5)$$

After crossing the perpendicular line of sight, the condition is identical to that described by Case C.

The four cases may be generalized:

$$D = (y + V) = \frac{x R_z \sin \phi \cos (\beta + \gamma)}{\sin (\alpha + \beta + \gamma + \phi)} \left[ \frac{1 + \sin (\beta + \gamma) \cos (\alpha + \beta + \gamma + \phi) \csc \theta}{f \sin \theta + x \cos (\beta + \gamma) \cos (\alpha + \beta + \gamma + \phi)} + \frac{x'}{f \sin (\alpha + \beta + \gamma + \phi) + x' \cos (\alpha + \beta + \gamma + \phi)} \right]$$

where  $x$  and  $x'$  are the components of displacement on the left and right of the optic axis, respectively.

The general equation reduces to the four special cases in the following manner:

Case A  $x' = 0$

Case B  $x' = 0$  and  $x = f \tan (\beta + \gamma)$

Case C  $x = f \tan (\beta + \gamma)$

Case D  $x = f \tan (\beta + \gamma)$  and  $x' = f \cot (\alpha + \beta + \gamma + \phi)$

The rigorous solutions may, in practice, be greatly simplified. If the optic axis is very nearly perpendicular to the line of displacement:

$$\sin (\alpha + \beta + \gamma + \phi) \approx 1$$

$$\cos (\alpha + \beta + \gamma + \phi) \approx 0$$

and the general equation reduces to:

$$D \approx \frac{x R_2 \sin \phi \cos (\beta + \gamma)}{f} \left[ \frac{1}{\sin \theta} + x' \right]$$

Depending upon photographic factors such as focal length and object distance, the simplified relation attains a degree of accuracy within the limits of camera resolution.

Other special cases have arisen in connection with the displacement of objects in two dimensions. In several instances two objects have been photographed with the same camera and, in general, the objects do not lie on the same line of displacement. In relating film displacement to spatial displacement in terms of the same known parameters as used in the foregoing cases, the trigonometric equations become exceedingly involved. However, the analytic procedure outlined above may be followed for variations of the problem.

It is obvious that symmetry about the optic axis and symmetry about a line of displacement perpendicular to the optic axis exist and the derived equations apply in all four "quadrants."

Although a discussion of object height is in opposition to the "two-dimensional" hypothesis, the film analysis provides a check on the

supposedly known object height. Figure 3 illustrates the spatial relation.

$$\frac{R_p}{\sin \phi} = \frac{R_z}{\sin \theta} , \quad f/g = \cos (\beta + \gamma) \quad (1a, 1b)$$

$$H = R_p \ h/g \quad (2)$$

Substituting:

$$H = h R_z \frac{\sin \phi \cos (\beta + \gamma)}{f \sin \theta} \quad (3)$$

where:

$h$  = measured film height of object

$H$  = true spatial height of object

### III. Three-Dimensional Displacement of A Point

An extension of the photogrammetric analysis to three dimensions was necessitated by experiments on Operation Ivy. The displacement of an object at an altitude high in comparison to the location of the nuclear detonation occurs in three dimensions, whereas the recorded displacement is, of course, in two dimensions on the film.

As in the two-dimensional case, the measured and true displacements are to be related to readily determined parameters. Figures 4 and 5 are the elevation and plan views, respectively, applicable to the following derivation.

Considering Figure 4:

$$g/f = \frac{i}{x + y} \quad (1)$$

$$(x + y) = n \cos (\epsilon + \theta) \quad (2)$$

or

$$i = \frac{g n \cos (\epsilon + \theta)}{f} \quad (3)$$

  
 $g$ ,  $n$  and  $f$  are known and  $(\epsilon + \theta)$  may be determined as follows:

$(\epsilon + \theta) = (\psi - \delta)$ , where  $\delta$  is known, but  $\psi$  is the projection of the vertical camera aiming angle,  $\rho$ , on the camera-object vertical plane.

The relation between  $\tan \rho$  and  $\tan \psi$ , wherein the two subject planes are separated by  $(\beta + \gamma)$  may be shown to be:

$$\tan \psi = \frac{\tan \rho}{\cos (\beta + \gamma)} \quad (4)$$

Relating  $j$  to  $i$  (Figure 4):

$$j = \frac{i \cos \epsilon}{\sin (\eta + \psi - \epsilon)} = \frac{g n \cos \epsilon \cos (\epsilon + \theta)}{f \sin (\eta + \psi - \epsilon)} \quad (5)$$

In (5),  $\psi$  is known from (4); similarly,  $\eta$  is the projection of the zero-object vertical angle,  $\xi$ , on the camera-object vertical plane. As in the derivation of (4):

$$\tan \eta = \frac{\tan \xi}{\cos \lambda} \quad (6)$$

where

$$\lambda = \alpha - (\beta + \gamma) + \phi \quad (\text{See Figure 5})$$

The angle  $\epsilon$  is known from:

$$\tan \epsilon = \tan (\epsilon + \theta) - g/f \quad (7)$$

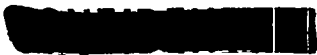
The component of motion,  $j$ , in the vertical camera-burst plane is now known. In a similar manner, the component of motion,  $m$ , in the horizontal plane is determined (Figure 5).

$$K/r = \frac{L}{r + s} \quad (8)$$

$$(r + s) = 0 \cos (\beta + \gamma) \quad (9)$$

or:

$$L = \frac{K0 \cos (\beta + \gamma)}{f} \quad (10)$$



Relating L to m:

$$m = \frac{L \cos \gamma}{\sin (\alpha + \phi - \gamma)} = \frac{KO \cos \gamma \cos (\beta + \gamma)}{f \sin (\alpha + \phi - \gamma)} \quad (11)$$

Angles  $\alpha$  and  $\phi$  are known and  $\gamma$  may be determined from:

$$\tan \gamma = \tan (\beta + \gamma) - K/f \quad (12)$$

From the known components of displacement, j and m, the true displacement, D, is determined from:

$$D = \left[ m^2 + j^2 \sin^2 \eta \right]^{1/2} \quad (13)$$

Substituting for m and j (from (5) and (11)):

$$D = \left\{ \left[ \frac{KO \cos \gamma \cos (\beta + \gamma)}{f \sin (\alpha + \phi - \gamma)} \right]^2 + \left[ \frac{g n \cos \epsilon \cos (\epsilon + \theta)}{f \sin (\eta + \psi - \epsilon)} \right]^2 \sin^2 \eta \right\}^{1/2} \quad (14)$$

Since K and g are the horizontal and vertical components of displacement on the film, they are related to the measured film displacement, d, by:

$$\begin{aligned} K &= d \sin \mu \\ g &= d \cos \mu \end{aligned} \quad (15)$$

where  $\mu$  is the angle between the displacement d and the vertical component g.

Since  $0 = n \cos \delta$ , (14) reduces, with substitution of (15), to:

$$D = \frac{nd}{f} \left\{ \left[ \frac{\sin \mu \cos \delta \cos \gamma \cos (\beta + \gamma)}{\sin (\alpha + \phi - \gamma)} \right]^2 + \left[ \frac{\cos \mu \cos \epsilon \sin \eta \cos (\psi - \delta)}{\sin (\eta + \psi - \epsilon)} \right]^2 \right\}^{1/2} \quad (16)$$

where:

$$\gamma = \tan^{-1} \left[ \tan (\beta + \gamma) - K/f \right]$$





$$\epsilon = \tan^{-1} \left[ \tan (\psi - \delta) - g/f \right]$$

$$\psi = \tan^{-1} \left[ \frac{\tan \rho}{\cos (\beta + \gamma)} \right]$$

$$\eta = \tan^{-1} \left[ \frac{\tan \xi}{\cos \lambda} \right]$$

$$\lambda = \alpha + \phi - (\beta + \gamma)$$

$$g = d \cos \mu$$

$$K = d \sin \mu$$

D = true spatial displacement

n = slant range, camera to initial position of object

d = measured film displacement

f = lens focal length

$\mu$  = angle between film displacement and vertical component thereof

$\delta$  = vertical angle, camera to initial position of object

$(\beta + \gamma)$  = horizontal camera aiming angle in relation to the initial position of object

$\rho$  = vertical camera aiming angle

$\xi$  = zero-object vertical angle

$\alpha$  = horizontal camera aiming angle

$\phi$  = horizontal angle, zero-camera and zero-object

In practice equation (16) may be greatly simplified if long focal length lenses are used and the camera is at a large distance from the object. Under these conditions, (16) may be shown to reduce to:

$$D = \frac{nd}{f} \left\{ \left[ \frac{\sin \mu \cos \delta}{\sin (\alpha + \phi)} \right]^2 + \left[ \frac{\cos \mu \sin \eta}{\sin (\delta + \eta)} \right]^2 \right\}^{1/2}$$



#### IV. Fireball Photogrammetry

Photogrammetric analysis, as applied to fireball measurements, falls into two main categories: surface burst, wherein the true zero point is known in advance and cameras are aimed accordingly, and air bursts, with the probability of the true burst point being off the optic axis.

##### A. Surface Burst

Figure 6 illustrates the relation between the true fireball radius and the apparent radius, as determined from film measurements. Earth curvature is not taken into account. From the figure:

$$\tan \alpha = R_a/R = r_a/f \quad (1)$$

$$\cos \alpha = R_t/R_a \quad (2)$$

and

$$R_t = (R_a f / f) \cos (\tan^{-1} r_a / f) \quad (3)$$

where:

$R_t$  = true fireball radius

$r_a$  = apparent fireball radius on film

$R$  = range from camera to zero

$f$  = lens focal length

For all practical purposes, this correction need be applied only to data from stations close to the fireball; in general, the camera is at such a large range that the correction is of the order of 0.05%, a negligible percentage at the present state of the technique for measuring the film data. Of course, for cameras used at long range, the surface at the detonation point is not seen and a correction for the curvature of the earth must be applied to the observed radius.

**CONFIDENTIAL**

A further source of discrepancy between true and apparent fireball radii is atmospheric refraction. No attempt will be made here to evaluate such effects; however, the order of magnitude has been observed to be about 5 feet displacement in 20 miles for atmospheric conditions such as those encountered on Operation Ivy.

### B. Air Burst

The problems associated with an air burst are:

- (a) The true location of the burst, determined by photographic triangulation.
- (b) The magnification factor between image and object when the object is not on the optic axis.
- (c) The true radius (or diameter) versus the apparent radius (or diameter).
- (d) The distortion of the image due to the off-axis burst.

#### a) Triangulation

Figure 7 shows two photo stations in relation to planned ground zero and the true ground zero. The angles  $\beta_1$  and  $\beta_2$  are determined from film measurements by:

$$\tan \beta_1 = d_1/r_1$$

$$\tan \beta_2 = d_2/r_2$$

Angles  $\alpha_1$  and  $\alpha_2$  are known from the camera aiming;  $\gamma_1$  and the distance between the two stations,  $D$ , are known from surveyed coordinates.

$$\psi = 90 - (\alpha_2 + \beta_2 + \gamma_1) \quad (1)$$

$$\phi = (\gamma_1 + \alpha_1 + \beta_1) \quad (2)$$

$$X = \frac{D \sin \psi}{\sin (\phi + \psi)} \quad (3)$$

and

$$Y = \frac{D \sin \phi}{\sin (\phi + \psi)} \quad (4)$$

From which follow:

$$Z = X \cos (\alpha_1 + \beta_1) \tag{5}$$

$$V = X \sin (\alpha_1 + \beta_1) \tag{6}$$

As a check, the second station provides:

$$W = Y \sin (\alpha_2 + \beta_2) \tag{7}$$

$$U = Y \cos (\alpha_2 + \beta_2) \tag{8}$$

Substituting (1) and (2) in (3) and (4) and applying (3) and (4) to (5) and (6), the full form of the equations expressing the coordinate distances of true ground zero from the two stations are:

Station 1	{	$Z = D \frac{\cos (\alpha_1 + \beta_1) \cos (\alpha_2 + \beta_2 + \gamma_1)}{\cos (\alpha_2 + \beta_2 - \alpha_1 - \beta_1)}$	North
		$V = D \frac{\sin (\alpha_1 + \beta_1) \cos (\alpha_2 + \beta_2 + \gamma_1)}{\cos (\alpha_2 + \beta_2 - \alpha_1 - \beta_1)}$	East
Station 2	{	$W = D \frac{\sin (\alpha_2 + \beta_2) \sin (\alpha_1 + \beta_1 + \gamma_1)}{\cos (\alpha_2 + \beta_2 - \alpha_1 - \beta_1)}$	South
		$U = D \frac{\cos (\alpha_2 + \beta_2) \sin (\alpha_1 + \beta_1 + \gamma_1)}{\cos (\alpha_2 + \beta_2 - \alpha_1 - \beta_1)}$	East

Having located true ground zero, the height of the burst above this point may be determined. Referring to Figure 8:

- X is known from the foregoing analysis
- ε is the vertical camera aiming angle (above the horizontal reference plane)
- E is the change in elevation above sea level between true ground zero and the camera
- C is the earth curvature in distance X
- H is the height of the burst above the horizontal plane
- H' is the true height of burst above the ground

$$\tan \rho = h/f, \quad \tan \eta = \tan (\epsilon - \rho) = H/X \quad (1)$$

$$H = X \left[ \frac{\tan \epsilon - h/f}{1 + h/f \tan \epsilon} \right] \quad (2)$$

$$H' = H + E + C \quad (3)$$

Strictly speaking, the burst height is the perpendicular to the earth's surface but, since curvature is small for camera ranges of the order of several miles, the difference between the true height and that given by Equation (3) is negligible.

b) Magnification Factor

Figure 9 shows plan and elevation views for deriving the magnification factor. In the figure:

- C = camera location
- A = planned burst point
- B = actual burst point
- R<sub>1</sub> = ground range to planned burst point
- R<sub>2</sub> = ground range to actual burst point
- α = angle between optic axis and actual burst point, in plan
- β = vertical camera aiming angle

The magnification factor is:  $R_{Oa}/f$  where

$$R_{Oa} = R_g + R_3 + R_4$$

$$R_g = \frac{R_1}{\cos \beta} \quad (1)$$

$$R_3 = \frac{\Delta}{\cos \beta} \quad (2)$$

$$R_4 = (H_B - H_{B_p} - X) \sin \beta \quad (3)$$

Adding (1), (2), and (3) and simplifying:

$$R_{oa} = \frac{R_1 + \Delta}{\cos \beta} + (H_B - H_{B_p} - X) \sin \beta \quad (4)$$

But:

$$X = \frac{\Delta \sin \beta}{\cos \beta} \quad (5)$$

$$H_{B_p} = \frac{R_1 \sin \beta}{\cos \beta} + H_c \quad (6)$$

$$R_1 + \Delta = R_2 \cos \alpha \quad (7)$$

Substituting (5), (6), and (7) in (4) and simplifying:

$$R_{oa} = R_2 \cos \alpha \cos \beta + (H_B - H_c) \sin \beta \quad (8)$$

c) Apparent Radius vs. True Radius

Figures 10 and 11 show the vertical and horizontal projections for an off-axis air burst. The burst occurs at a height  $\Delta h_v$  above the planned burst height, a distance  $\Delta E$  away from the planned vertical object plane of the camera and a distance  $\Delta S$  to the right of the vertical plane of the optic axis. These errors in burst position will result in a measured film radius which is larger than the true radius. The magnitude of the image error is proportional to the magnitude of the off-axis burst error.

Furthermore, an image radius measured horizontally does not equal that measured vertically, again due to the off-axis character of the burst position.

Considering the vertical radii:

$$\frac{dv_1}{f} = \tan (\gamma_v - \beta) \quad (1)$$

$$\frac{dv_2}{f} = \tan (\epsilon_v - \beta) \quad (2)$$

~~CONFIDENTIAL~~

The fireball radius, as measured on the film, is then:

$$\Delta d_v = d_{v2} - d_{v1} = f \left[ \tan (\epsilon_v - \beta) - \tan (\gamma_v - \beta) \right] \quad (3)$$

But:

$$\epsilon_v = \gamma_v + \phi_v \quad (4)$$

Substituting (4) in (3) and simplifying:

$$\Delta d_v = f \left\{ \frac{\tan \phi_v \left[ 1 + \tan^2 \beta \tan^2 \gamma_v + \tan^2 \gamma_v + \tan^2 \beta \right]}{\left[ 1 + \tan \gamma_v \tan \beta \right] \left[ 1 - \tan \gamma_v \tan \phi_v + \tan \beta \tan \gamma_v + \tan \beta \tan \phi_v \right]} \right\} \quad (5)$$

Solving for  $\tan \phi_v$ :

$$\tan \phi_v = \frac{\Delta d_v \left[ 1 + \tan \beta \tan \gamma_v \right]^2}{f \left[ 1 + \tan^2 \beta \tan^2 \gamma_v + \tan^2 \gamma_v + \tan^2 \beta \right] - \Delta d_v \left[ \tan \beta - \tan \gamma_v \right] \left[ 1 + \tan \gamma_v \tan \beta \right]} \quad (6)$$

But:

$$\sin \phi_v = \frac{R_{fv}}{R_{sv}} \quad (7)$$

where:

$$R_{sv} = \frac{h + \Delta h_v}{\sin \gamma_v} \quad (8)$$

Therefore:

$$\phi_v = \sin^{-1} \left[ \frac{R_{fv} \sin \gamma_v}{h + \Delta h_v} \right] \quad (9)$$

Since the sine and tangent of  $\phi_v$  are known,  $\phi_v$  may be eliminated and a relation found between  $\Delta d_v$  and  $R_{fv}$ . In the right triangle defined by  $\tan \phi_v$  and  $\sin \phi_v$ :

$$(A \Delta d_v D R_{fv})^2 + (Bf - C \Delta d_v)^2 D^2 R_{fv}^2 = (A \Delta d_v)^2 \quad (10)$$

where, for algebraic simplification:

$$\begin{aligned} A &= (1 + \tan \beta \tan \gamma_v)^2 \\ B &= (1 + \tan^2 \beta \tan^2 \gamma_v + \tan^2 \gamma_v + \tan^2 \beta) \\ C &= (\tan \beta - \tan \gamma_v)(1 + \tan \gamma_v \tan \beta) \\ D &= \frac{\sin \gamma_v}{h + \Delta h_v} \end{aligned}$$

Solving (10) for  $R_{fv}$  :

$$R_{fv} = \frac{A \Delta d_v}{D \left[ (A^2 + C^2) \Delta d_v^2 - 2BCf \Delta d_v + B^2 f^2 \right]^{1/2}} \quad (11)$$

Equation (11) relates the measured film fireball radius to the true fireball radius. The fireball radius in the object plane, as normally determined from the film measurement is, however:

$$R_{av} = M/f \Delta d_v \quad (12)$$

where  $M/f$  is the magnification factor of section b. In the notation used in Figures 10 and 11:

$$M = (R_{sh} \cos \alpha_h + \Delta E) \cos \beta + (h + \Delta h_v) \sin \beta \quad (13)$$

Relating apparent fireball radius to true fireball radius through (11) and (12):

$$R_{fv} = \frac{A R_{av}}{DM \left[ \left( \frac{A^2 + C^2}{M^2} \right) R_{av}^2 - 2BC/M R_{av} + B^2 \right]^{1/2}} \quad (14)$$

Equation (14) may be simplified in practice: if, as is usually the case, the camera is at a range very large compared to the fireball radius (i.e.,  $M \gg R_{av}$ ), equation (14) reduces to:

$$R_{fv} = R_{av} \cos (\gamma_v - \beta) \quad (15)$$

~~CONFIDENTIAL~~

Moreover, if the burst occurs on the optic axis (i.e.,  $\gamma_v = \beta$ ), the apparent radius is equal to the true radius.

When applying the general equation (14) to a specific case it is necessary to evaluate  $M$  as a function of  $R_{ah}$  in order to determine whether the simplified relation may be valid. In some instances the burst will be much closer to a given camera station, and the data from that station should be corrected by the general equation to give the true radius, whereas other camera stations are far enough from the burst that the simplified equation may be used.

Although the equations have been derived for a specific burst location, symmetry about the optic axis implies, and may readily be shown, that the equations are valid regardless of the location of the burst with respect to the planned burst position.

The derivation for the horizontal radius proceeds in the same fashion as that for the vertical radius, resulting in:

$$R_{rh} = \frac{R_{ah}}{\frac{M}{R_{sh}} \left[ \left( \frac{J^2+1}{M^2} \right) R_{ah}^2 + \frac{2IJ}{M} R_{ah} + I^2 \right]^{1/2}} \quad (16)$$

where:

$$M = (R_{sh} \cos \alpha_h + \Delta E) \cos \beta + (h + \Delta h_v) \sin \beta$$

$$J = \tan \alpha_h$$

$$I = \frac{1 + \tan^2 \alpha_h}{\cos \beta (1 + \tan \gamma_v \tan \beta)}$$

If  $M \gg R_{ah}$ , equation (16) reduces to:

$$R_{rh} = R_{ah} \cos \alpha_h \quad (17)$$

and, if the burst is on-axis ( $\alpha_h = 0$ )

$$R_{rh} = R_{ah} = R_{rv} = R_{af} \quad (18)$$

~~CONFIDENTIAL~~

~~CONFIDENTIAL~~

d) Distortion of Image Due to Geometry

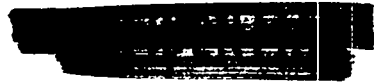
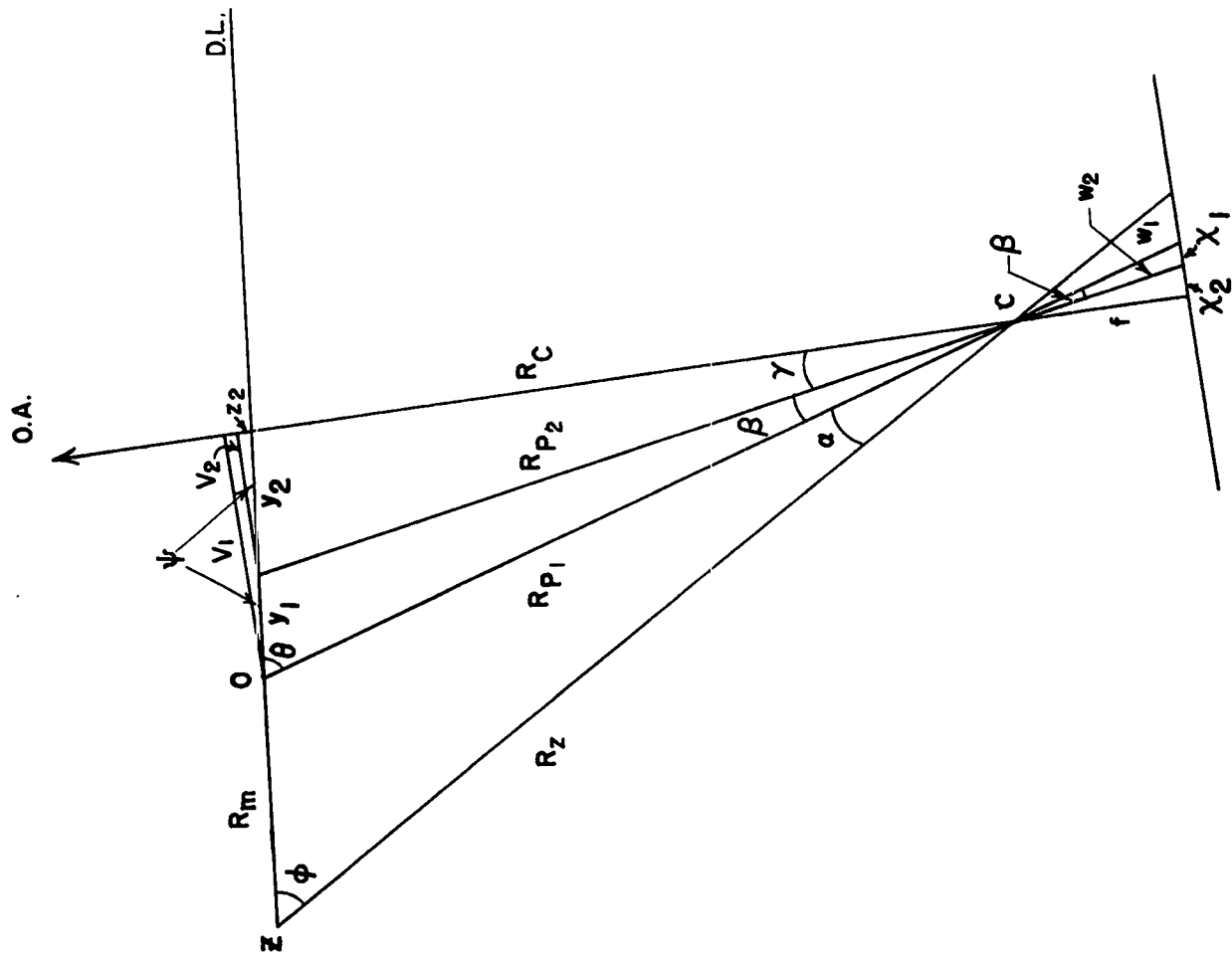
Although the general equations (14) and (16) indicate very serious distortions of the fireball image when the camera is close to the burst, the most frequently encountered conditions, represented by equations (15) and (17), also give evidence of distorted fireball images. A detailed study of this distortion is felt to be unnecessary at this time for several reasons.

Lens distortion has been assumed negligible in the foregoing analyses; toward the edge of the film frame this distortion is probably comparable to that produced by off-axis objects. Moreover, the current method of measuring fireball radius consists of fitting a circular grid to the fireball image; since, at least in the early stages, the fireball is not spherical, the smoothing afforded by the grid method probably overshadows the distortion. Numerical examples have been worked with the derived equations and, in general, show a deviation of true radius from apparent radius of the order of several tenths of a per cent; scatter of data is greater than this error. Until such time as the variation in data can be reduced, the radius correction is felt to be unnecessary for most of the film data; special occasions may arise in which the full corrections should be applied.

~~CONFIDENTIAL~~



FIG. 1





~~CONFIDENTIAL~~

UNCLASSIFIED

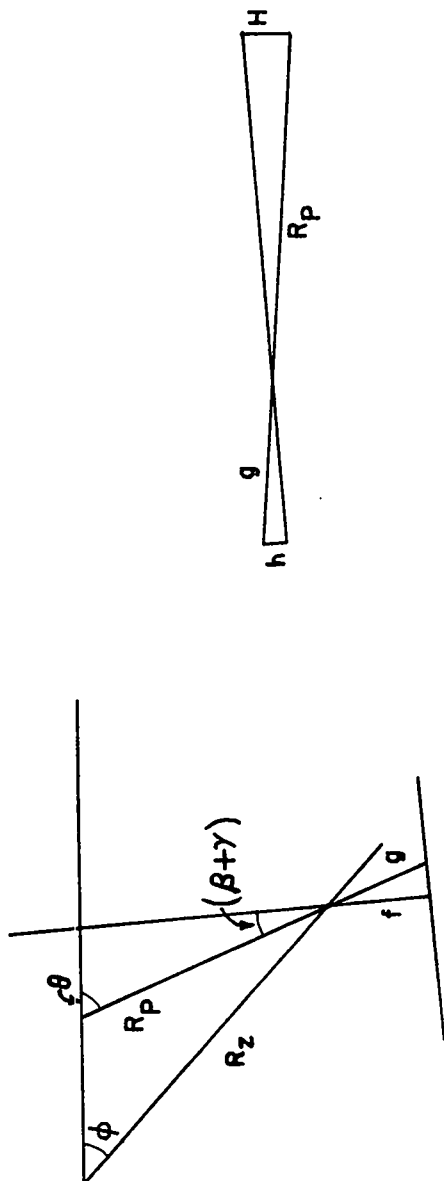


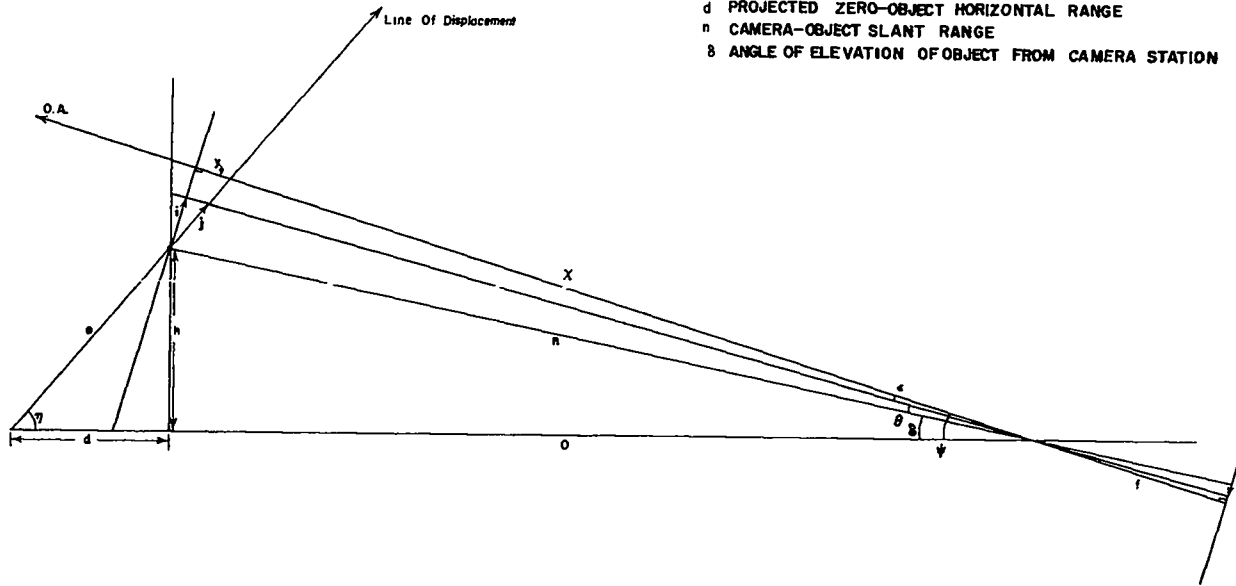
FIG. 3

UNCLASSIFIED

~~CONFIDENTIAL~~

UNCLASSIFIED

-29-



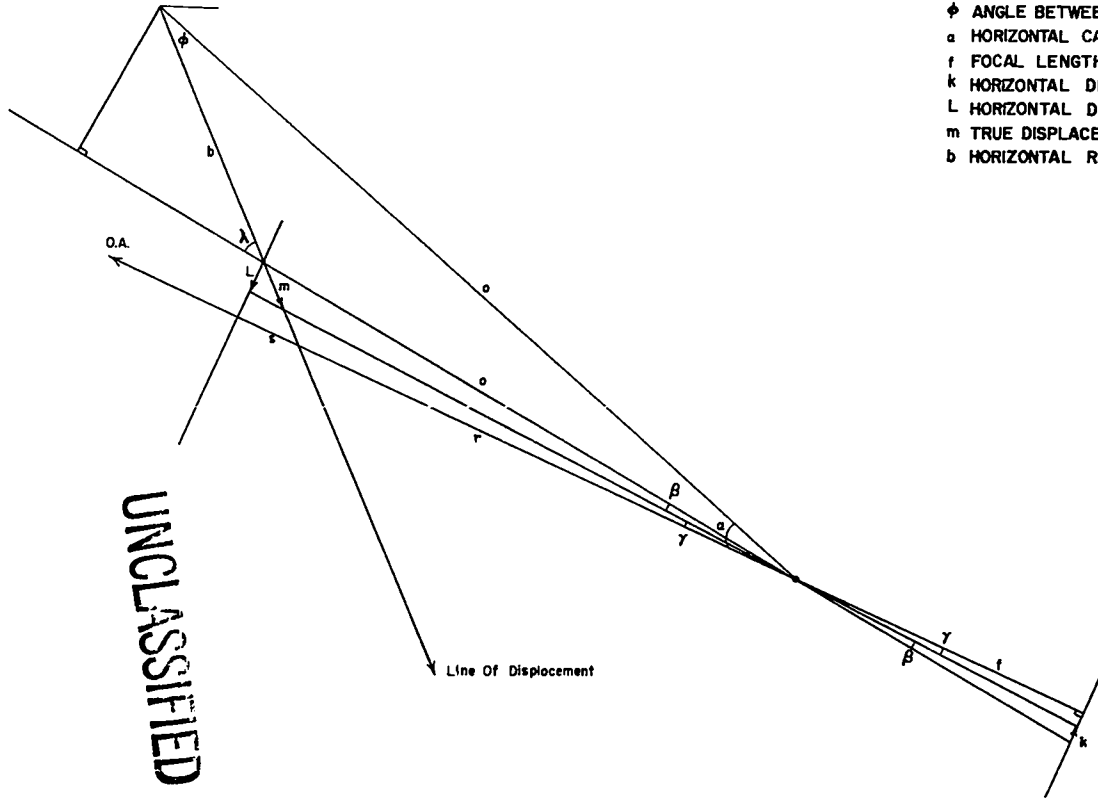
ELEVATION  
VERTICAL PLANE THROUGH INITIAL POSITION OF OBJECT CONTAINING OBJECT-CAMERA LINE

- $\psi$  VERTICAL CAMERA AIMING ANGLE (PROJECTED),  $\rho$  TRUE AIMING ANGLE
- $f$  FOCAL LENGTH
- $\gamma$  PROJECTED ZERO-OBJECT VERTICAL ANGLE,  $\xi$  TRUE ZERO-OBJECT VERTICAL ANGLE
- $h$  HEIGHT OF OBJECT
- $v$  VERTICAL DISPLACEMENT ON FILM
- $l$  VERTICAL DISPLACEMENT IN OBJECT PLANE
- $j$  TRUE DISPLACEMENT IN ELEVATION
- $e$  PROJECTED ZERO-OBJECT RANGE
- $d$  PROJECTED ZERO-OBJECT HORIZONTAL RANGE
- $n$  CAMERA-OBJECT SLANT RANGE
- $\theta$  ANGLE OF ELEVATION OF OBJECT FROM CAMERA STATION

FIG. 4

UNCLASSIFIED

UNCLASSIFIED



PLAN  
 HORIZONTAL PLANE THROUGH INITIAL POSITION OF OBJECT

- $\phi$  ANGLE BETWEEN ZERO-CAMERA AND ZERO-OBJECT
- $\alpha$  HORIZONTAL CAMERA AIMING ANGLE
- $f$  FOCAL LENGTH
- $k$  HORIZONTAL DISPLACEMENT ON FILM
- $L$  HORIZONTAL DISPLACEMENT IN OBJECT PLANE
- $m$  TRUE DISPLACEMENT IN PLAN
- $b$  HORIZONTAL RANGE ZERO-OBJECT

FIG. 5

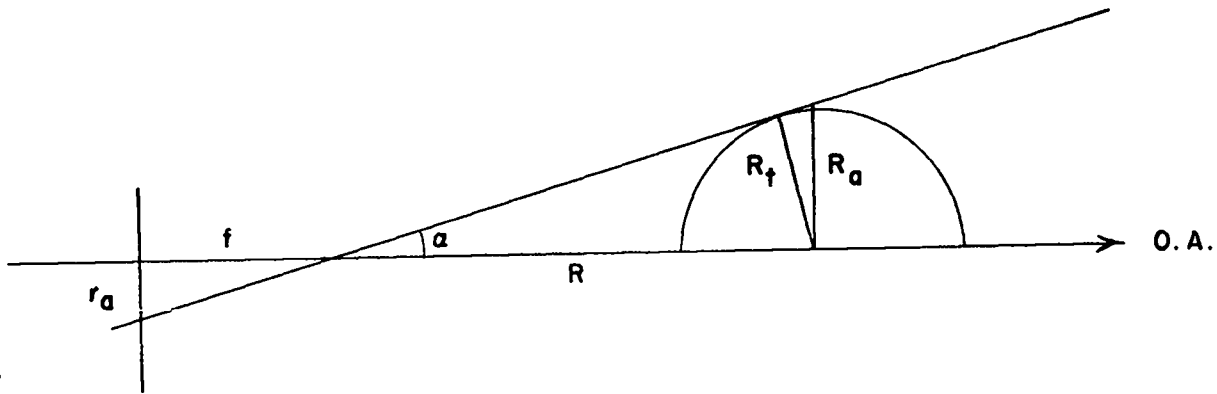


FIG. 6

UNCLASSIFIED

UNCLASSIFIED

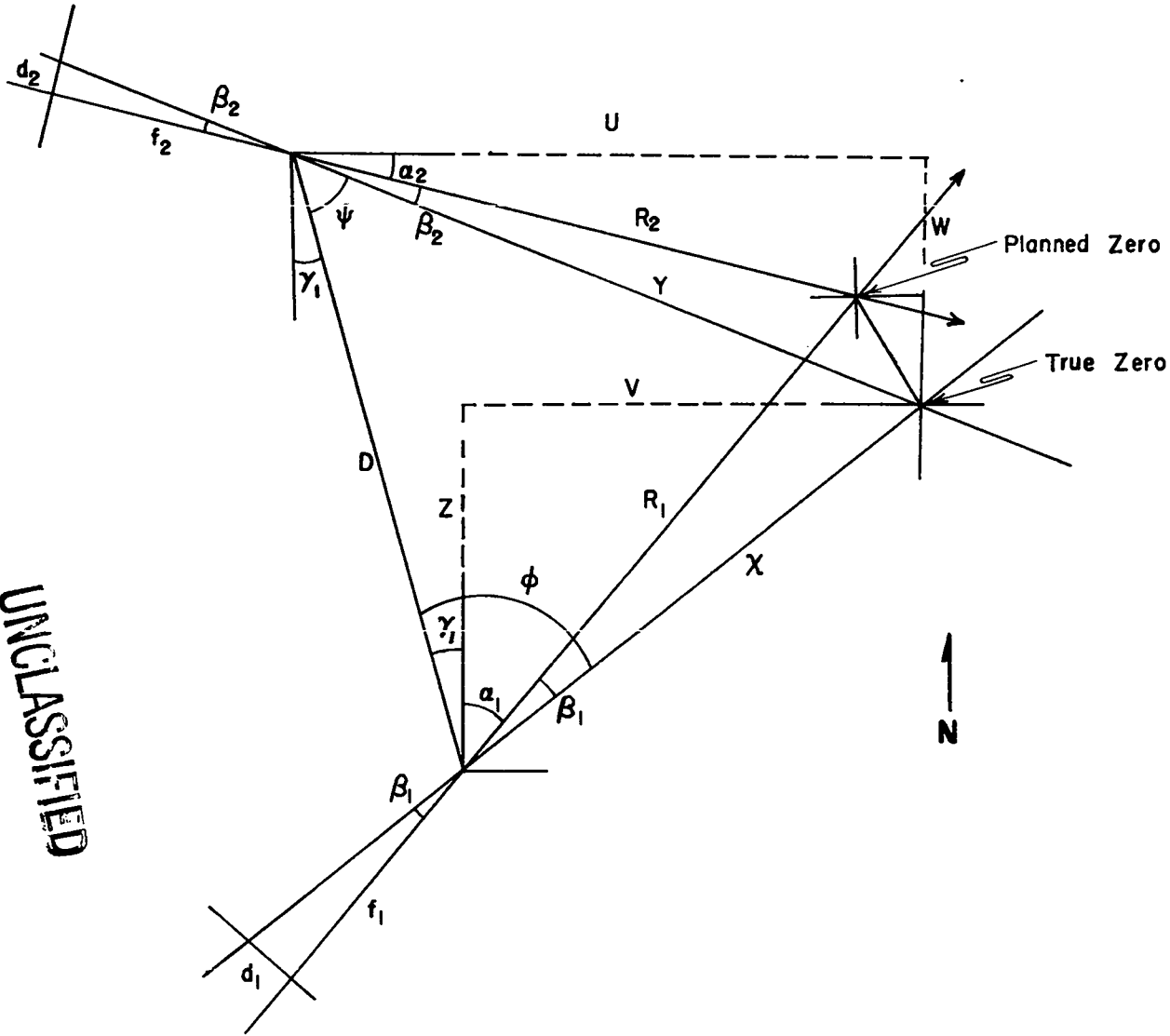


FIG. 7

UNCLASSIFIED



UNCLASSIFIED

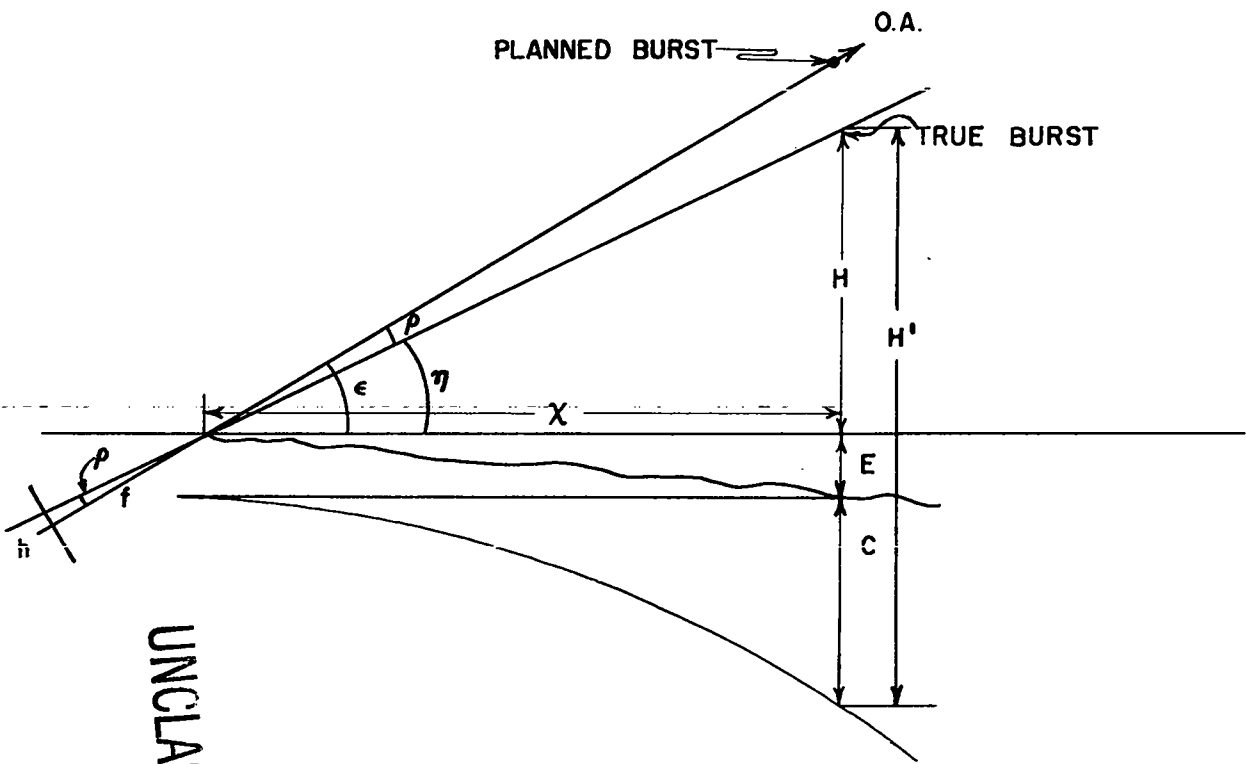


FIG. 8

UNCLASSIFIED



UNCLASSIFIED

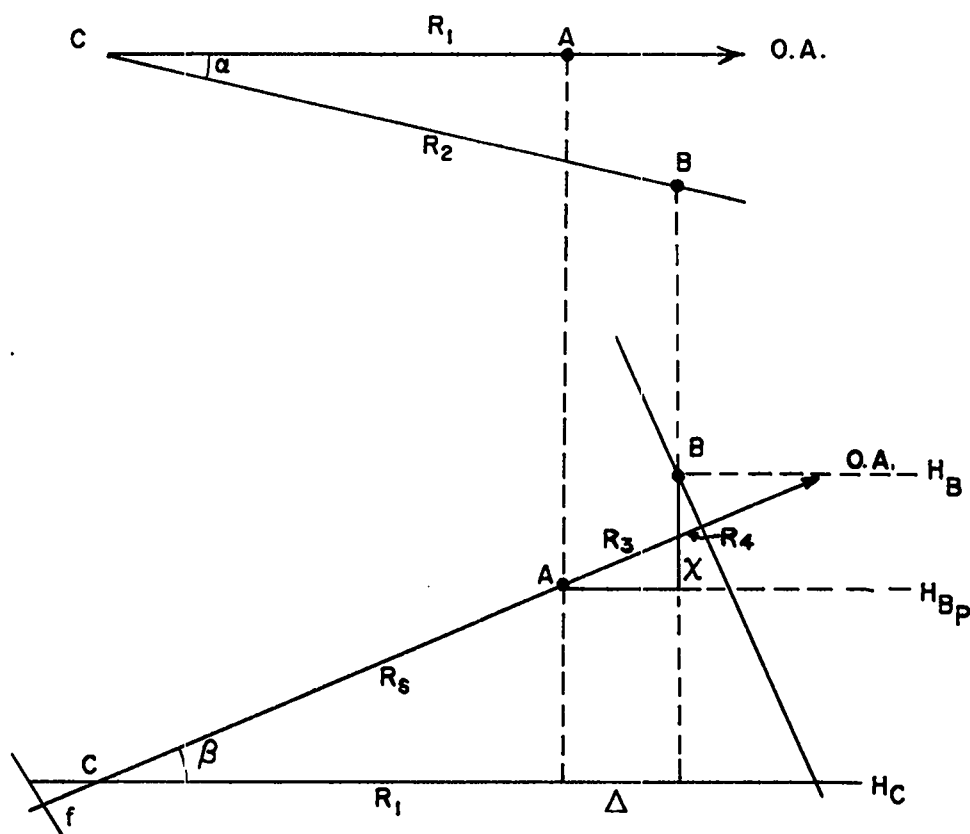


FIG. 9

UNCLASSIFIED

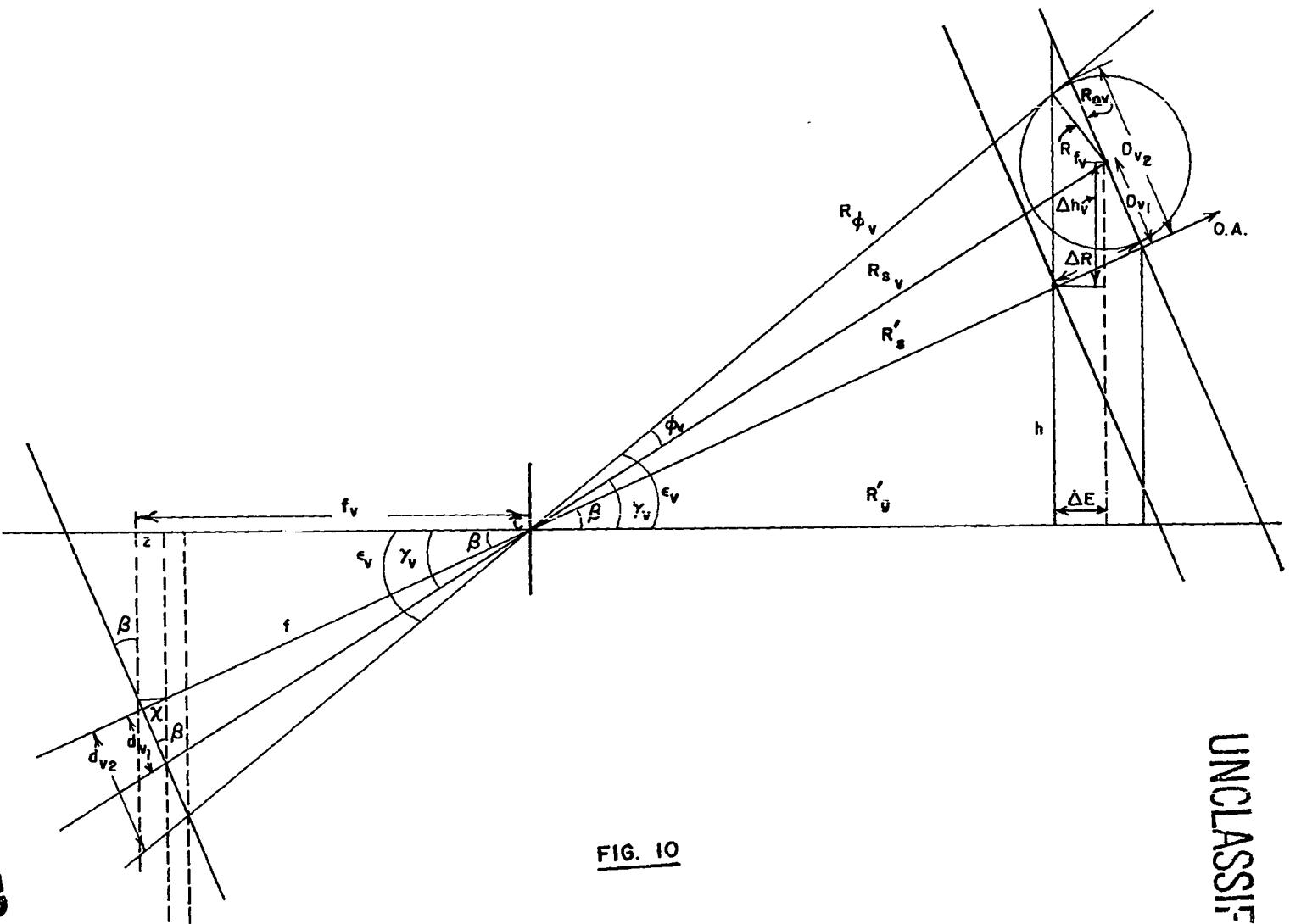


FIG. 10

UNCLASSIFIED

UNCLASSIFIED



UNCLASSIFIED

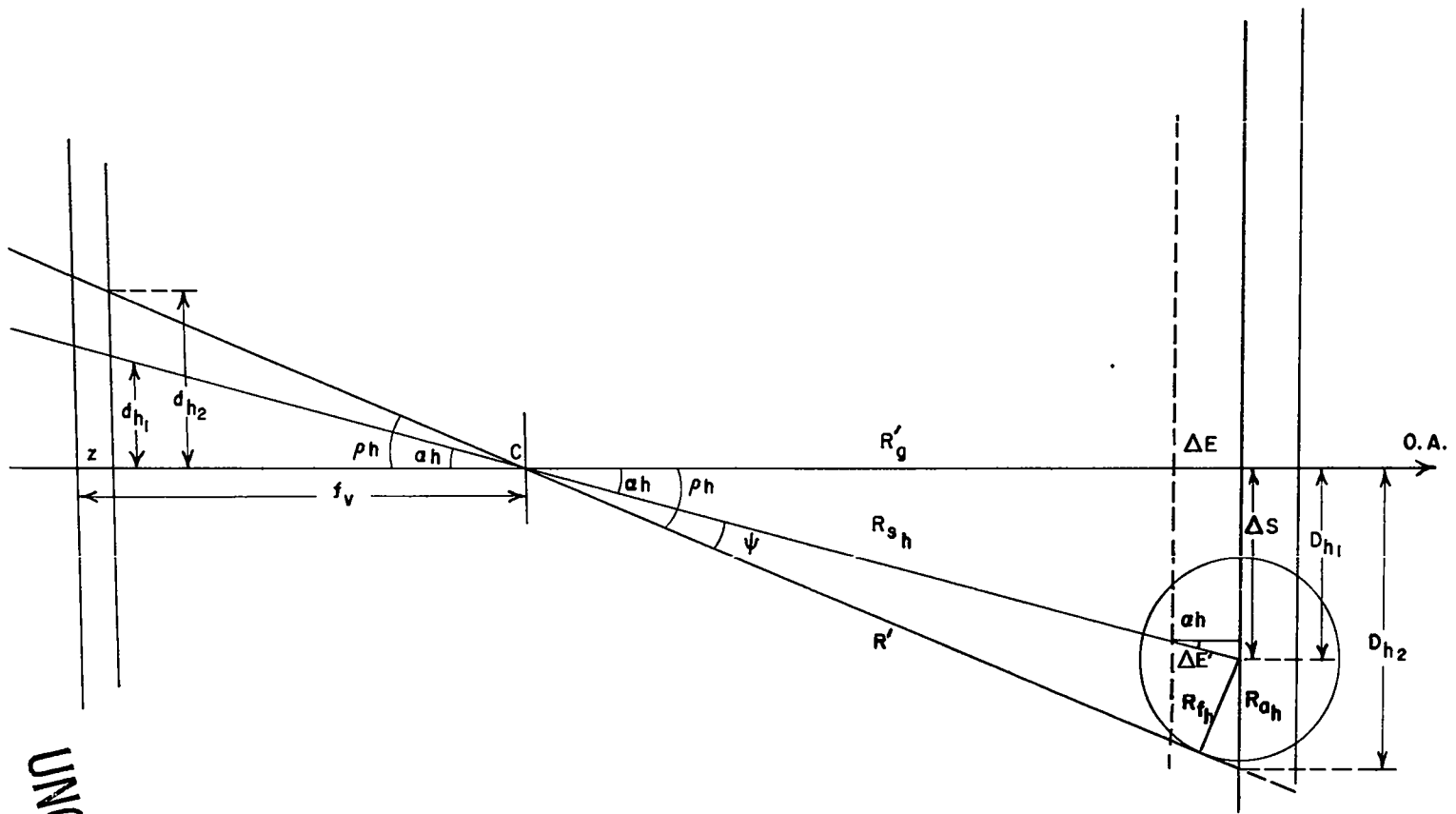


FIG. 11

UNCLASSIFIED



**REPORT LIBRARY**

JUN 10 1955